



## Combining Heliostat Solar Energy and Reverse Osmosis: Thermoeconomic Analysis for Power Generation and Freshwater Production

Seyyed Masoud Seyyedi<sup>1,2,\*</sup>, Seyyed Mostafa Ghadami<sup>2,3</sup>

<sup>1</sup>Department of Mechanical Engineering, Ali. C., Islamic Azad University, Aliabad Katoul, Iran

<sup>2</sup>Energy Research Center, Aliabad Katoul Branch, Islamic Azad University, Aliabad Katoul, Iran

<sup>3</sup>Department of Electrical Engineering, Ali. C., Islamic Azad University, Aliabad Katoul, Iran

Article info	Abstract
<p><b>Keywords:</b></p> <p>Solar energy Heliostat Reverse Osmosis Power Generation Freshwater Production Thermoeconomic</p> <hr/> <p><b>Article history:</b></p> <p>Received: 16 06 2025 Accepted: 24 06 2025</p>	<p>The simultaneous generation of electricity and fresh water has become an increasingly important objective in modern energy system design, particularly in regions facing water scarcity and growing energy demand. The integration of renewable energy sources with desalination technologies offers a sustainable and environmentally friendly approach to meeting these challenges. Among renewable options, solar energy—especially in the form of concentrated solar power—provides high potential for large-scale applications. In this study, a hybrid system consisting of a heliostat solar field coupled with a reverse osmosis (RO) desalination unit is investigated for the cogeneration of electricity and fresh water. A detailed thermodynamic analysis is first performed to evaluate the performance of the proposed system. The thermodynamic properties at all state points, including mass flow rate, temperature, pressure, and enthalpy, are calculated to analyze energy conversion processes and losses within individual components and the overall system. This analysis forms the basis for an accurate assessment of system efficiency. Subsequently, a thermoeconomic analysis is conducted to estimate the unit costs of electricity and desalinated water, enabling a direct link between technical performance and economic feasibility. The effects of various design, environmental, and economic parameters on system profitability are systematically examined. The design variables include the pressure ratio of the air compressor, the efficiencies of the gas turbine and air compressor, and the number of heliostats in the solar field. Environmental parameters such as ambient air temperature and solar direct normal irradiance (DNI) are considered due to their strong influence on solar energy availability and system output. In addition, economic factors, including the interest rate and the economic lifetime of system components, are analyzed to evaluate long-term financial performance. The results indicate that increasing the number of heliostats significantly enhances system profitability. At a compressor pressure ratio of 6, the maximum profit reaches 582.5, 841.7, and 1093 \$/h for 1800, 2200, and 2600 heliostats, respectively. Moreover, as DNI increases from 750 W/m<sup>2</sup> to 910 W/m<sup>2</sup>, the fresh water production rate rises from 166.6 m<sup>3</sup>/h to 194 m<sup>3</sup>/h, corresponding to a 16.4% increase. From an economic standpoint, reducing the interest rate from 12% to 10% for an economic lifetime of 25 years leads to a substantial profit increase from 841.7 \$/h to 1310 \$/h, highlighting the strong impact of economic parameters on the overall viability of the system.</p>

\* Corresponding author.

E-mail address: [s.masoud\\_seyyedi@iau.ac.ir](mailto:s.masoud_seyyedi@iau.ac.ir) (S.M. Seyyedi).

## 1. Introduction

Simultaneous production of electricity and fresh water is a basic need in most remote areas. Solar energy can be applied to power generation directly using photovoltaic (PV) solar cells or indirectly using a solar thermal system [1]. Due to the shortage of fresh water in the world, fresh water is produced using seawater. There are various methods for producing fresh water as shown in Fig. 1 [2]. Many researchers have tried to provide cogeneration systems for producing electricity and fresh water. In 2010, a combined solar organic Rankine cycle with reverse osmosis desalination process was proposed by Nafey and Sharaf [3]. They performed energy and exergy analysis and cost evaluations for their proposed cycle. In 2016, exergoeconomic analysis of a solar farm coupled with a two-stage direct reverse osmosis (RO) system has been conducted by Mokhtari et al. [4]. In 2016, Yari et al. [5] proposed a novel cogeneration system for producing power and fresh water using solar energy. In 2016, Noorpoor et al. [6] examined exergy analysis and optimization of a multi-generation system for electricity, heating, cooling and fresh water, where solar energy and sugarcane biomass were used. In 2017, a cogeneration system based on a series two-stage organic Rankine cycle integrated with a reverse osmosis desalination (RO) unit was proposed Nemati et al. [7]. The system produced the consumed electricity and fresh water of a ship. In 2017, integration of an eco-design strategy for small RO desalination system driven by photovoltaic energy was performed by Monnot et al. [8]. In 2018, the thermodynamic performance of a solar-based multi-generation system designed to produce hydrogen, cooling, heating, and freshwater was evaluated by Yilmaz [9]. In 2019, Farsi and Dincer [10] extended a multigeneration system driven by a geothermal source for generating power, hydrogen, cooling and freshwater. In 2020, the waste energy of a steam power plant was employed for the production of fresh water by Ghorbani et al. [11]. Solar collectors and auxiliary boilers were applied for providing the required heat for the steam power plant. In 2020, exergoeconomic and exergoenvironmental analyses of a desalination plant

were conducted by Lourenço and Carvalho [12]. Their system consists of an internal combustion engine, a Rankine-based heat recovery unit, and a seawater RO system. In 2020, Ghorbani et al. [13] proposed a hybrid renewable energy system for production of power and fresh water using parabolic trough solar collectors. The system produced electricity (459.9 MW) and freshwater (3628 kgmol/h). In 2020, Mohammadi et al. [14] designed a gas turbine combined cycle to produce electricity, cooling and freshwater. In 2020, a renewable-based energy system was proposed by Lourenço and Carvalho [15]. Their system produced electricity and fresh water. In 2020, Mohammadi et al. [16], evaluated several hybrid trigeneration configurations based on a gas turbine combined cycle for generating electricity, cooling and freshwater. In 2021, comprehensive techno-economic analysis of a compressed air energy storage hybridized with solar and desalination units was performed by Alirahmi et al. [17]. In 2022, thermoeconomic analysis for a combined solar energy system with RO desalination unit was performed by Assareh et al. [18]. In 2022, Yuksel et al. [19] proposed a solar-fed multigeneration plant that provided power, freshwater, cooling, methane, ammonia, hydrogen and urea. It consisted of a PTC field, a steam Rankine cycle, an ORC, a RO unit, an absorption chiller, a hydrogen compression system, a PEM electrolyzer, as well as ammonia, methane, and urea generation systems. The energy and exergy efficiencies was determined at 66.12%, and 61.56%, respectively and the cost of producing hydrogen was 1.94 \$/kg. In 2024, an integrated energy system was proposed by Abouzied et al. [20]. It included three subsystems: a biogas-fired GTC, a modified S-CO<sub>2</sub> recompression cycle for supplementary electricity generation, and a MED unit for distilled water production.

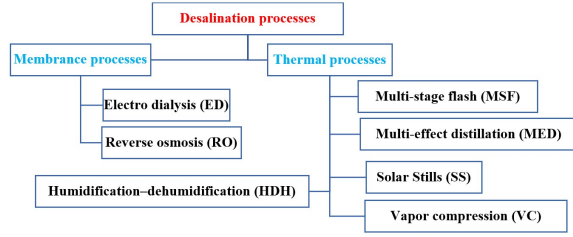


Fig.1: Different methods of water desalination [2]

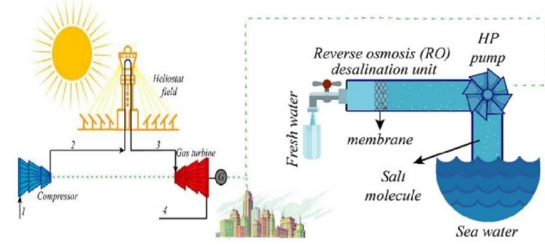


Fig. 2: Schematic view of the proposed combined system

## 2. Reverse osmosis unit (RO)

RO is a physical process that uses the osmosis phenomenon, that is, the osmotic pressure difference between the salt water and the pure water to remove the salts from water [21]. In 1996, Malek et al. [22] provided a realistic economic model that relates the various operational and capital cost elements to the design variable values. In 2011, a good review article was written by Pangarkar and Sane [23]. In 2012, a RO desalination process with multiple-feed and multiple-product was investigated by Lu et al. [24]. In 2014, a multi-objective optimization of RO networks for seawater desalination was proposed by Du et al. [25]. In 2017, for the desalination system, Blanco-Marigorta et al. [26] reviewed the exergy efficiencies of several RO systems, which varied between 2% to 92%.

## 3. System descriptions

Heliostat is generally referred to a set of mirrors that are located around a rotating axis and reflect sunlight to a central receiver. Fig. 2 shows a schematic view of the proposed combined system that consists of an air compressor, a solar heliostat field (to generate hot air), a gas turbine (to generate power) and a RO distillation unit (to produce fresh water). In first, the air enters the air compressor and is compressed, and then it is heated after passing through the solar heliostat field. Hot air enters the gas turbine to generate power, while the outlet is still at a high temperature. A part of the produced electricity is sold to the grid and another part is consumed by the desalination unit to produce fresh water.

## 4. Mathematical Modeling

The mass and energy balance equations for each component must be written. Also, an economic model must be developed.

### 4.1. Thermodynamic analysis

#### ➤ Air compressor (AC):

The outlet temperature of air compressor can be calculated by [27]:

$$T_2 = T_1 \left[ 1 + \frac{1}{\eta_{AC}} \left( \left( \frac{P_2}{P_1} \right)^{\frac{k-1}{k}} - 1 \right) \right] \quad (1)$$

The air compressor work is calculated as follows:

$$\dot{W}_{AC} = \dot{m}_1 c_{p,air} (T_2 - T_1) \quad (2)$$

#### ➤ Solar Heliostat field (SHF):

The total amount of solar energy in heliostats is given by Eqs. (3) and (4) [2].

$$\dot{Q}_{sun} = A_{hel} \times N_{hel} \times DNI \quad (3)$$

$$\dot{Q}_h = \eta_{hel} \times \dot{Q}_{sun} \quad (4)$$

Heat losses can be quantified by Eq. (5).

$$\dot{Q}_{loss} = h_{air} A_h (T_r - T_0) + \sigma \epsilon A_h (T_r^4 - T_0^4) \quad (5)$$

$$h_{air} = 10.45 - v_{air} + 10\sqrt{v_{air}} \quad (6)$$

Finally, the heat transfer rate between air and receiver can be calculated by:

$$\dot{Q}_r = \dot{Q}_h - \dot{Q}_{loss} = \dot{m}_2 (h_3 - h_2) \quad (7)$$

#### ➤ Gas turbine (GT):

The outlet temperature of gas turbine can be calculated by [27]:

$$T_4 = T_3 \left[ 1 - \frac{1}{\eta_{GT}} \left( 1 - \left( \frac{P_3}{P_4} \right)^{\frac{1-k}{k}} \right) \right] \quad (8)$$

The gas turbine work is calculated as follows:

$$\dot{W}_{GT} = \dot{m}_3 c_{p,air} (T_3 - T_4) \quad (9)$$

The net work of solar power cycle is calculated as follows:

$$\dot{W}_{net} = \dot{W}_{GT} - \dot{W}_{AC} \quad (10)$$

The power consumption for the desalination unit pump (HP) is obtained by Eq. (11):

$$\dot{W}_{RO} = HP = \left( \frac{1000 \times M_f \times \Delta P}{3600 \times \rho_f \times \eta_p} \right) \quad (11)$$

The main equations required for modeling the RO unit are represented in [Appendix A](#). Here, the electrical fraction is define by:

$$\lambda = \dot{W}_{RO} / \dot{W}_{net} \quad (12)$$

$$\dot{W}_{grid} = (1 - \lambda)\dot{W}_{net} \quad (13)$$

#### 4.2. Thermo-economic analysis

Now, the thermo-economic model is presented. The cost rate of each component ( $\dot{Z}_k$ ) is given by [1]:

$$\dot{Z}_k = \frac{\varphi \times CRF \times PW}{\tau} \quad (14)$$

where the capital recovery factor (CRF) is a function of the lifetime of components ( $n$ ) and interest rate ( $i$ ) and can be calculated by:

$$CRF = \frac{i \times (i + 1)^n}{(i + 1)^n - 1} \quad (15)$$

Also, the operation time of the system and the coefficient operation are considered 12 hours per day (from 6 to 18) and 0.85, respectively. Therefore,  $\tau = 0.85 \times 12 \times 365 = 3723$  hr.

The present worth is defined as:

$$PW = TCI - SV(PWF) \quad (16)$$

where

$$PWF = \frac{1}{(i + 1)^n} \quad (17)$$

and

$$SV = \mu (TCI) \quad (18)$$

where  $\mu$  is the salvage percentage. Appendix A presents the total capital investment (TCI) cost for each component.

The average cost of electricity ( $c_W$  in \$/kWh) is obtained by:

$$c_W = (\dot{Z}_{AC} + \dot{Z}_{SHF} + \dot{Z}_{GT}) / \dot{W}_{net} \quad (19)$$

The average cost of fresh water ( $c_{FW}$  in \$/m<sup>3</sup>) is obtained by:

$$c_{FW} = (\dot{Z}_{RO} + c_W \times \dot{W}_{RO}) / M_d \quad (20)$$

Revenue ( $\dot{R}$ ) means money that can be earned from the sale of electricity and fresh water and can be calculated as follows:

$$\dot{R} = C_{sale.W} \times \dot{W}_{grid} + C_{sale.FW} \times M_d \quad (21)$$

where  $C_{sale.W} = 0.121$  \$/kwh and  $C_{sale.FW} = 3$  \$/m<sup>3</sup> [1]:

Finally, Profit can be obtained by:

$$\text{Profit} = \dot{R} - (\dot{Z}_{total} + \dot{Z}_{land}) \quad (22)$$

where

$$\dot{Z}_{total} = \dot{Z}_{AC} + \dot{Z}_{SHF} + \dot{Z}_{GT} + \dot{Z}_{RO} \quad (23)$$

and

$$\dot{Z}_{land} = 0.1 \times \dot{Z}_{total} \quad (24)$$

## 5. Results and discussion

Here, firstly a comparison between the present results with other works is presented and then the effects of the main parameters on the performance of the system are investigated.

### 5.1. Model validation

[Table 1](#) presents the predefined values for modeling the proposed system. Also, [Table 2](#) presents the obtained results based on the values of [Table 1](#). To model the proposed cogeneration system for electricity and fresh water production, an Engineering Equation Solver (EES) code was extended. The comparison between the obtained results for the RO desalination unit with the data reported by Nafey et al. [3] and Kianfard et al. [28] is outlined in [Table 3](#). The comparison shows a good agreement between the results.

**Table 1:** Modeling input parameters [1, 3, 18]

Parameter	Definition	Amount
<b>Power system</b>		
$T_0$	Ambient temperature	20 °C
$P_0$	Ambient pressure	101.3 kPa
$DNI$	Direct normal irradiance	850 W/m <sup>2</sup>
$N_{hel}$	Number of heliostats	2200
$A_r$	The area of heliostats	60 m <sup>2</sup>
$T_r$	The receiver local temperature	1000 °C
$T_3$	The gas turbine inlet temperature	750 °C
$\eta_{hel}$	Heliostat efficiency	0.71
$\epsilon_r$	Surface emissivity of the receiver	0.88
$v_w$	Wind speed	5 m/s
$r_p$	Compressor pressure ratio	6
$\eta_{GT}$	Gas turbine efficiency	0.85
$\eta_{AC}$	Air compressor efficiency	0.82
<b>RO unit</b>		
$T_f$	Feed water temperature	25 °C
$SR$	Salt rejection percentage	0.9944
$X_f$	Seawater salinity	45000 ppm
$n_m$	Number of elements	7
$C_{pv}$	Price of the pressure vessel	7000 \$
$FF$	Fouling factor	0.85
$RR$	Recovery ratio	0.30
$n_{pv}$	Number of pressure vessels	42
$C_k$	Each membrane price	1200 \$
$A_e$	Element area	35.4 m <sup>2</sup>
$\rho_f$	Density of fluid	1020 kg/m <sup>3</sup>
$\eta_p$	Pump efficiency	0.80
Element type	FTSW30HR-380	-
<b>Economic parameters</b>		
$\tau$	Working hour per year	3723 hr
$i$	Interest rate	0.12
$n$	Lifetime of components	25 year
$\phi$	Maintenance factor	1.06
$\mu$	Salvage percentage	15 %
$\lambda$	Electrical fraction	0.05
$c_{sale.elec}$	Selling price of electricity	0.12 \$/kWh
$c_{sale.FW}$	Selling price of fresh water	3 \$/m <sup>3</sup>

**Tables 2:** Results based on the values of Table 1

Parameter	Value
$\dot{W}_{RO}$	1578 kW
$\dot{W}_{grid}$	29979 kW
$\dot{W}_{net}$	31557 kW
$M_f$	613.3 m <sup>3</sup> /h
$M_d$	184 m <sup>3</sup> /h
$M_b$	429.3 m <sup>3</sup> /h
$\dot{Z}_T$	3034 \$/h
SPC	8.576 (kWh/m <sup>3</sup> )
$c_{cost.elec}$	0.0858 \$/kWh
$c_{cost.FW}$	2.515 \$/m <sup>3</sup>
Profit	841.7 \$/h

**Table 3:** Comparison between the present results with Refs. [3] and [28]

Variable (Unit)	Nafey and Sharaf [3]	Kianfard et al. [28]	Present work
SPC (kWh/m <sup>3</sup> )	7.680	8.01	7.766
HP(kW)	1131	1180	1132
$M_f$ (m <sup>3</sup> /h)	485.9	485.9	485.9
$M_b$ (m <sup>3</sup> /h)	340.1	340.12	340.13
$X_b$ (ppm)	64180	64150	64178
$X_d$ (ppm)	250	253	252
SR (-)	0.9944	0.9944	0.9944
$\Delta P$ (kPa)	6850	6845	6843.9

**5.2. Effects of active parameters**

Fig. 3 shows the values of profit versus pressure ratio of compressor at different values of number of heliostats. It discovers that the values of profit reach a maximum value at  $r_p = 6$ . The maximum values of profit are 582.5, 841.7 and 1093 \$/h for number of heliostats ( $N_{hel}$ ) 1800, 2200 and 2600, respectively at  $r_p = 6$ . Therefore, the profit increases from 582.5 \$/h to 1093 \$/h (87.6%) when the number of heliostats increases from 1800 to 2600 at optimum conditions.

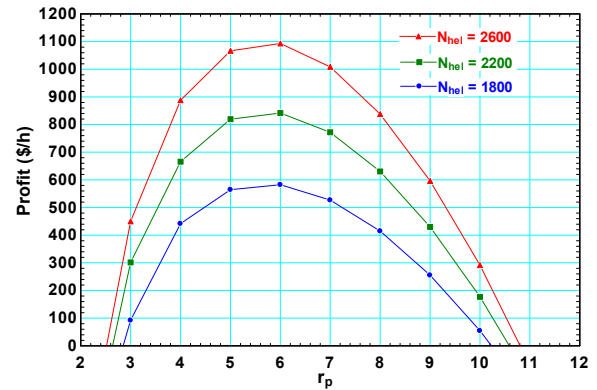


**Fig. 3:** Variations of profit versus  $r_p$  at different values of  $N_{hel}$

Fig. 4 demonstrates the amount of electricity sold to the grid ( $\dot{W}_{grid}$ ) and the amount of fresh water produced ( $M_d$ ) versus pressure ratio of compressor at  $N_{hel} = 2200$ . It is interesting to note that the maximum values for  $\dot{W}_{grid}$  and  $M_d$  occur at  $r_p = 7$  while the maximum value of profit occurs at  $r_p = 6$ . These values are 30438 kW and 185.9 m<sup>3</sup>/h at  $r_p = 7$ .

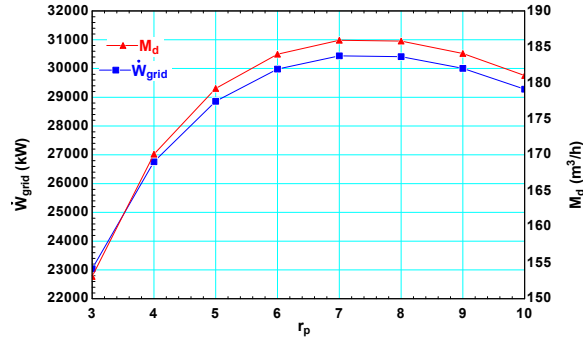


Fig. 4: Variations of  $\dot{W}_{grid}$  and  $M_d$  versus  $r_p$

Fig. 5 shows the cost of electricity ( $c_{cost,elec}$ ) and the cost of fresh water ( $c_{cost,FW}$ ) versus pressure ratio of compressor. Here, the minimum values for  $c_{cost,elec}$  and  $c_{cost,FW}$  occur at  $r_p = 5$ . The minimum values are 0.0856 \$/kWh and 2.51 \$/m<sup>3</sup> at  $r_p = 5$ . These values are less than the selling price of electricity and selling price of fresh water in Table 1. Figures 3, 4 and 5 emphasizes that the objective function must be clearly defined during optimization.

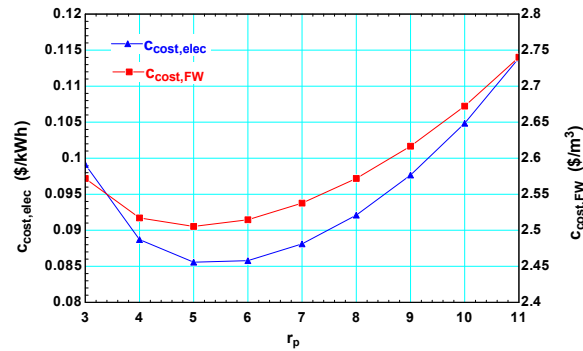


Fig. 5: Variations of  $c_{cost,elec}$  and  $c_{cost,FW}$  versus  $r_p$

Fig. 6 presents the variations of  $\dot{W}_{grid}$  and  $M_d$  versus direct normal irradiance (DNI). As it can be seen, these values increase with increasing DNI. For example, the values of  $\dot{W}_{grid}$  increase from 25976 kW to 32381 kW (24.6% increasing) and  $M_d$  increases from 166.6 m<sup>3</sup>/h to 194 m<sup>3</sup>/h (16.4% increasing) as DNI goes up from 750 W/m<sup>2</sup> to 910 W/m<sup>2</sup>.

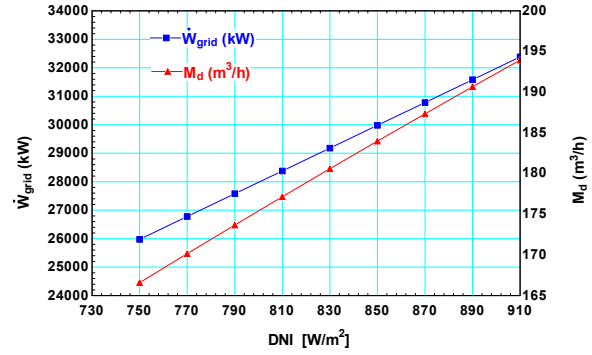


Fig. 6: Variations of  $\dot{W}_{grid}$  and  $M_d$  versus DNI

Fig. 7 shows the variations of  $c_{cost,elec}$  and  $c_{cost,FW}$  versus direct normal irradiance (DNI). As it can be seen, these values decrease with increasing DNI. For example, the value of  $c_{cost,elec}$  decreases from 0.0966 \$/kWh to 0.0806 \$/kWh (16.5% decreasing) and  $c_{cost,FW}$  decreases from 2.576 \$/m<sup>3</sup> to 2.485 \$/m<sup>3</sup> (3.5% decreasing) as DNI goes up from 750 W/m<sup>2</sup> to 910 W/m<sup>2</sup>.

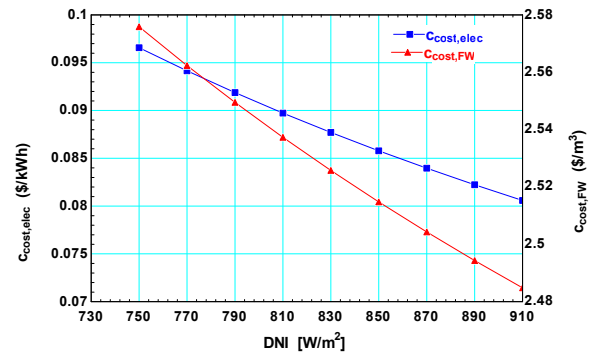


Fig. 7: Variations of  $c_{cost,elec}$  and  $c_{cost,FW}$  versus DNI

Fig. 8 presents a comparison between the values of profit for different values of direct normal irradiance at three different values of gas turbine efficiency ( $\eta_{GT}$ ) and air compressor efficiency ( $\eta_{AC}$ ). The figure discovers that the values of profit increase with increasing the values of  $\eta_{GT}$  and  $\eta_{AC}$ . For example, the value of profit increases from 841.7 \$/h to 1028 \$/h (22.1% increasing) when  $\eta_{GT}$  ascends from 0.85 to 0.88 at  $DNI = 850$  W/m<sup>2</sup>. Also, the value of profit increases from 841.7 \$/h to 931 \$/h (10.6% increasing) when  $\eta_{AC}$  ascends from 0.82 to 0.85 at  $DNI = 850$  W/m<sup>2</sup>.

Also, Table 4 represents the exact values associated with Fig. 8.

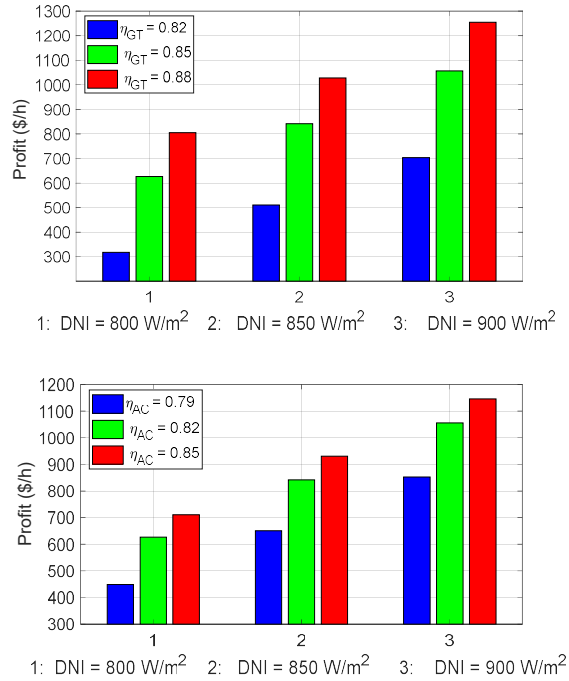


Fig. 8: Variations of profit for various values of DNI at different values of  $\eta_{GT}$  and  $\eta_{AC}$

Table 4: The values of Profit (\$/h) at different values of DNI,  $\eta_{GT}$  and  $\eta_{AC}$

	DNI (W/m <sup>2</sup> )		
	800	850	900
$\eta_{GT}$			
0.82	317.6	510.8	703.8
0.85	626.8	841.7	1056
0.88	805.3	1028	1255
$\eta_{AC}$			
0.79	448.4	650.8	853.0
0.82	626.8	841.7	1056
0.85	710.3	931.0	1146

Tables 5 and 6 show the values of  $\dot{W}_{grid}$  and  $M_d$  for different values of direct normal irradiance at three different values of gas turbine efficiency ( $\eta_{GT}$ ). These tables discover that the values of  $\dot{W}_{grid}$  and  $M_d$  increase with increasing the values of  $\eta_{GT}$ . For example, the values of  $\dot{W}_{grid}$  increase from 29979 kW to 33348 kW (11.2% increasing) when  $\eta_{GT}$  ascends from 0.85 to 0.88 at  $DNI = 850 \text{ W/m}^2$ . Also, the values of  $M_d$  increase from 184 m<sup>3</sup>/h to 197.9 m<sup>3</sup>/h (7.5%

increasing) when  $\eta_{GT}$  ascends from 0.85 to 0.88 at  $DNI = 850 \text{ W/m}^2$ .

Table 5: The values of  $\dot{W}_{grid}$  (kW) at different values of DNI and  $\eta_{GT}$

	DNI (W/m <sup>2</sup> )		
	800	850	900
$\eta_{GT}$			
0.82	24834	26611	28387
0.85	27977	29979	31981
0.88	31121	33348	35574

Table 6: The values of  $M_d$  (m<sup>3</sup>/h) at different values of DNI and  $\eta_{GT}$

	DNI (W/m <sup>2</sup> )		
	800	850	900
$\eta_{GT}$			
0.82	161.4	169.4	177.2
0.85	175.4	184.0	192.3
0.88	188.8	197.9	206.7

Fig. 9 presents the variations of  $M_d$  versus seawater salinity ( $X_f$ ) at different values of  $N_{hel}$ . The figure shows that the values of  $M_d$  decrease with increasing  $X_f$  for each value of  $N_{hel}$ . For example, the value of  $M_d$  decreases from 201 m<sup>3</sup>/h to 170 m<sup>3</sup>/h (15.4% decreasing) when  $X_f$  goes up from 40000 ppm to 49000 ppm at  $N_{hel} = 2200$ .

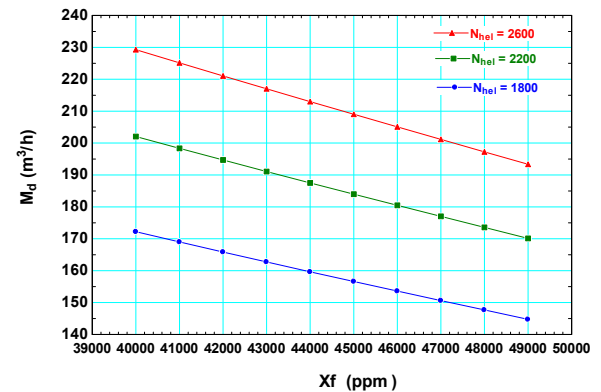


Fig. 9: variations of  $M_d$  versus  $X_f$  at different values of  $N_{hel}$

Fig. 10 demonstrates the effects of the lifetime of the system ( $n$ ) and interest rate ( $i$ ) on the profit. The CRF increases by ascending of  $i$  and  $n$  (see, Eq. (15)) and therefore, the cost of each component increases. The result is less profit. Profit increases when the values of  $n$  ascend for each value of  $i$ . Also, profit increases with

decreasing  $i$  for a constant value of a  $n$ . For example, the value of profit increases from 235.2 \$/h to 409.9 \$/h (74.3% increasing) when  $n$  increases from 20 to 29 years for  $i = 14\%$ . Also, the value of profit increases from 841.7 \$/h to 1310 \$/h (55.6% increasing) when  $i$  decreases from 12% to 10% for  $n = 25$ .

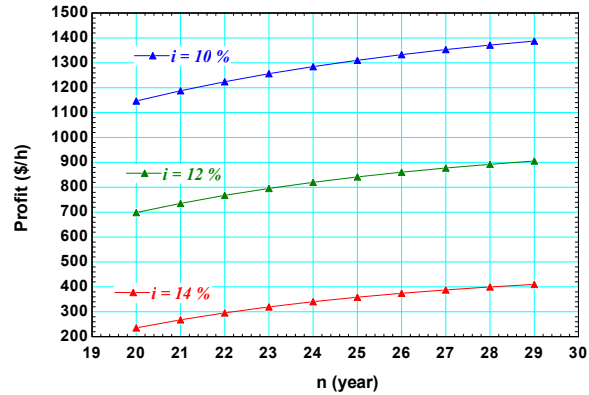


Fig. 10: Variations profit versus the lifetime of the system ( $n$ ) at three different values of interest rate ( $i$ )

## 6. Conclusion

In the present work, a heliostat solar farm was combined with a reverse osmosis desalination unit to produce electricity and fresh water. Modeling of the system was performed in EES software. The main results can be summarized as follows:

- The maximum values of profit are 582.5, 841.7 and 1093 \$/h for number of heliostats ( $N_{hel}$ ) 1800, 2200 and 2600, respectively at  $r_p = 6$ .
- The values of  $\dot{W}_{grid}$  and  $M_d$  increase 24.6% and 16.4%, respectively, as  $DNI$  goes up from  $750 \text{ W/m}^2$  to  $910 \text{ W/m}^2$ .
- The minimum values for  $c_{cost.elec}$  and  $c_{cost.fw}$  occur at  $r_p = 5$ .
- The value of profit increases 22.1% when  $\eta_{GT}$  ascends from 0.85 to 0.88 at  $DNI = 850 \text{ W/m}^2$ .
- The value of profit increases 10.6% when  $\eta_{AC}$  ascends from 0.82 to 0.85 at  $DNI = 850 \text{ W/m}^2$ .
- The value of  $M_d$  decreases from 15.4% when  $X_f$  goes up from 40000 ppm to 49000 ppm at  $N_{hel} = 2200$ .

- The value of profit increases 55.6% when interest rate decreases from 12% to 10% for  $n = 25$ .

## References

- [1] SM. Seyyedi, M. Hashemi-Tilehnoee, M. Sharifpur, Thermoeconomic analysis of a solar-driven hydrogen production system with proton exchange membrane water electrolysis unit, Thermal Science and Engineering Progress, 30 (2022) 101274.
- [2] SM. Seyyedi, SM. Ghadami, Integration of a solar heliostat field with humidifier-dehumidifier desalination units to generate electricity and fresh water, Journal of Renewable Energy and Smart Systems Vol. 1, No. 1, 2024: 81-92
- [3] A.S.Nafey, M.A.Sharaf, Combined solar organic Rankine cycle with reverse osmosis desalination process: Energy, exergy, and cost evaluations, Renewable Energy 35 (2010) 2571-2580
- [4] Hamid Mokhtari, Hossein Ahmadisedigh, Iman Ebrahimi, Comparative 4E analysis for solar desalinated water production by utilizing organic fluid and water, Desalination 377 (2016) 108–122
- [5] M. Yari, A.E. Mazareh, A.S. Mehr, A novel cogeneration system for sustainable water and power production by integration of a solar still and PV module, Desalination 398 (2016 Nov 15) 1.
- [6] Noorpoor, A., Heidarnejad, P., Hashemian, N. and Ghasemi, A. (2016) 'A thermodynamic model for energetic performance and optimization of a solar and biomass-fuelled multigeneration system', Energy Equipment and Systems, Vol. 4, No. 2, pp.281–289.
- [7] Arash Nemati, Mohsen Sadeghi, Mortaza Yari, Exergoeconomic analysis and multi-objective optimization of a marine engine waste heat driven RO desalination system integrated with an organic Rankine cycle using zeotropic working fluid, Desalination 422 (2017) 113–123
- [8] M. Monnot, G.D. Carvajal, S. Laborie, C. Cabassud, R. Lebrun, Integrated approach in eco-design strategy for small RO desalination plants powered by photovoltaic energy, Desalination (2017 Jun 9).
- [9] Yilmaz F. Thermodynamic performance evaluation of a novel solar energy based multigeneration system. Appl Therm Eng 2018;143:429-437. <https://doi.org/10.1016/j.applthermaleng.2018.07.125>.

- [10] Farsi Aida, Dincer Ibrahim. Development and evaluation of an integrated MED/membrane desalination system. *Desalination* 2019;463:55–68.
- [11] B. Ghorbani, R. Shirmohammadi, M. Mehrpooya, Development of an innovative cogeneration system for fresh water and power production by renewable energy using thermal energy storage system, *Sustainable Energy Technologies and Assessments* 37 (2020) 100572
- [12] Atilio B. Lourenço, Monica Carvalho, Exergoeconomic and exergoenvironmental analyses of an off-grid reverse osmosis system with internal combustion engine and waste heat recovery, *Chemical Engineering Journal Advances* 4 (2020) 100056
- [13] Ghorbani B, Mahyari KB, Mehrpooya M, Hamed MH. Introducing a hybrid renewable energy system for production of power and fresh water using parabolic trough solar collectors and LNG cold energy recovery. *Renew Energy* 2020;148:1227-1243. <https://doi.org/10.1016/j.renene.2019.10.063>.
- [14] Mohammadi K, Khaledi MSE, Saghafifar M, Powell K. Hybrid systems based on gas turbine combined cycle for trigeneration of power, cooling, and freshwater: a comparative techno-economic assessment. *Sustain Energy Technol Assessments* 2020;37:100632. <https://doi.org/10.1016/J.SETA.2020.100632>.
- [15] Atilio Barbosa Lourenço, Monica Carvalho, Exergy, exergoeconomic and exergy-based emission cost analyses of a coconut husk-fired power and desalination plant, *Int. J. Exergy*, Vol. 32, No. 3, 2020
- [16] Kasra Mohammadi, Mohammad Saeed Efati Khaledi, Mohammad Saghafifar, Kody Powell, Hybrid systems based on gas turbine combined cycle for trigeneration of power, cooling, and freshwater: A comparative techno-economic assessment, *Sustainable Energy Technologies and Assessments* 37 (2020) 100632
- [17] Alirahmi SM, Bashiri Mousavi S, Razmi AR, Ahmadi P. A comprehensive techno-economic analysis and multi-criteria optimization of a compressed air energy storage (CAES) hybridized with solar and desalination units. *Energy Convers Manag* 2021;236:114053. <https://doi.org/10.1016/J.ENCONMAN.2021.114053>.
- [18] Ehsanolah Assareh, Mostafa Delpisheh, Seyed Mojtaba Alirahmi, Sirous Tafi, Monica Carvalho, Thermodynamic-economic optimization of a solar-powered combined energy system with desalination for electricity and freshwater production, *Smart Energy* 5 (2022) 100062
- [19] Yunus Emre Yuksel, Murat Ozturk, and Ibrahim Dincer, “Design and analysis of a new solar hydrogen plant for power, methane, ammonia and urea generation,” *International Journal of Hydrogen Energy*, vol. 47, pp. 19422–19445, 2022.
- [20] Amr S. Abouzied, Sarminah Samad, Azher M. Abed, Mohamed Shaban, Fahad M. Alhomayani, Shirin Shomurotova, Mohammad Sediq Safi, Raymond Ghandour, Yasser Elmasry, Albara Ibrahim Alrawashdeh, Efficient thermal integration model based on a biogas-fired gas turbine cycle (GTC) for electricity and desalination applications; thermo-economic and GA-based optimization, *Case Studies in Thermal Engineering* 64 (2024) 105492
- [21] T. Younos and K. E. Tulou, “Overview of desalination techniques,” *Journal of Contemporary Water Research and Education*, vol. 132, no. 3, p. 10, 2005.
- [22] A. Malek, M.N.A. Hawlader, Design and economics of RO seawater desalination, *Desalination* 105 (1996) 245–261.
- [23] B.L. Pangarkar, M. G. Sane, M. Guddad, Reverse Osmosis and Membrane Distillation for Desalination of Groundwater: A Review, *International Scholarly Research Network, ISRN Materials Science*, Volume 2011, Article ID 523124, 9 pages, doi:10.5402/2011/523124
- [24] Y. Lu, A. Liao, Y. Hu, The design of reverse osmosis systems with multiple-feed and multiple-product, *Desalination* 307 (2012) 42–50
- [25] Yawei Du, Lixin Xie, Jie Liu, Yuxin Wang, Yingjun Xu, Shichang Wang, Multi-objective optimization of reverse osmosis networks by lexicographic optimization and augmented epsilon constraint method, *Desalination* 333 (2014) 66–81
- [26] A.M. Blanco-Marigorta, A. Lozano-Medina, J.D. Marcos, A critical review of definitions for exergetic efficiency in reverse osmosis desalination plants, *Energy* 137 (2017) 752–760, doi: 10.1016/j.energy.2017.05.136 .
- [27] S.M. Seyyedi, M. Hashemi-Tilehnoee, M.A. Rosen, “Exergy and exergoeconomic analyses of a novel integration of a 1000 MW pressurized water reactor power plant and a gas turbine cycle through a superheater”, *Annals of Nuclear Energy* 115 (2018) 161–172.

[28] Hossein Kianfard, Shahram Khalilarya, Samad Jafarmadar, Exergy and exergoeconomic evaluation of hydrogen and distilled water production via combination of PEM electrolyzer, RO desalination unit and geothermal driven dual fluid ORC, *Energy Conversion and Management* 177 (2018) 339–349

## Appendix A

**Table A:** Modeling of RO unit [3,28].

Description	Equation
The feed mass flow rate ( $M_f$ )	$M_f = M_d/RR$
The distillate product salt concentration ( $X_d$ )	$X_d = X_f \times (1 - SR)$
The rejected brine ( $M_b$ )	$M_b = M_f - M_d$
The rejected salt concentration ( $X_b$ ) in $\frac{\text{kg}}{\text{m}^3}$	$X_b = \frac{M_f \times X_f - M_d \times X_d}{M_b}$
The temperature correction factor ( $TCF$ )	$TCF = \exp \left[ 2700 \left( \frac{1}{T + 273} - \frac{1}{298} \right) \right]$
The membrane water permeability ( $k_w$ )	$k_w = \frac{6.84 \times 10^{-8} (18.6865 - 0.177 \times X_b)}{T + 273}$
The osmotic pressure for feed side ( $\pi_f$ ), brine side ( $\pi_b$ ), and distillate product side ( $\pi_d$ )	$\pi_f = 75.84 \times X_f$ $\pi_b = 75.84 \times X_b$ $\pi_d = 75.84 \times X_d$
The average osmotic pressure on the feed side ( $\pi_{ave}$ )	$\pi_{ave} = 0.5 \times (\pi_f + \pi_b)$
The net osmotic pressure across the membrane ( $\Delta\pi$ )	$\Delta\pi = \pi_{ave} - \pi_d$
The net pressure difference across the membrane ( $\Delta P$ )	$\Delta P = \left( \frac{M_d}{3600 \times TCF \times FF \times A_e \times n_m \times n_{pv} \times k_w} \right) + \Delta\pi$
The required power input in kW to the RO driving pump (HP)	$\dot{W}_{RO} = \text{HP} = \left( \frac{1000 \times M_f \times \Delta P}{3600 \times \rho_f \times \eta_p} \right)$
The specific power consumption (SPC) in $\frac{\text{kWh}}{\text{m}^3}$	$\text{SPC} = \frac{\text{HP}}{M_d}$

## Appendix B

The total capital investment (TCI) cost for each component is represented in Table B.

**Table B:** Economic cost equations for the components [1,2, 22]

Component	Purchase cost equation	Ref. year	Cost index
Air Compressor (AC)	$TCI_{AC} = 71.1 \times \dot{m}_1 \left( \frac{1}{0.9 - \eta_{AC}} \right) \left( \frac{P_2}{P_1} \right) \ln \left( \frac{P_2}{P_1} \right)$	1994	368.1
Gas Turbine (GT)	$TCI_{GT} = 479.3 \times \dot{m}_3 \left( \frac{1}{0.92 - \eta_{GT}} \right) \ln \left( \frac{P_3}{P_4} \right) [1 + \exp(0.036 \times T_3 - 54.4)]$	1994	368.1
Solar Heliostat Field (SHF)	$TCI_{hel} = 150 \times A_{hel} \times N_{hel}$ $TCI_{rec} = A_{rec} \times (79 \times T_{rec} - 42000)$ $TCI_{RO} = n_m \times n_{pv} \times C_k + n_{pv} \times C_{pv} + 996 \times (M_f)^{0.8} + TCI_{HPP}$	2014	576.1
RO unit*	$\begin{cases} TCI_{HPP} = 52(Q_{HPP} \times P_{HPP}) & \text{where category (A): } Q_{HPP} \leq 200 \text{ m}^3/\text{h} \\ TCI_{HPP} = 81(Q_{HPP} \times P_{HPP})^{0.96} & \text{where category (B): } 200 \text{ m}^3/\text{h} < Q_{HPP} < 450 \text{ m}^3/\text{h} \\ TCI_{HPP} = 393000 + 10710 \times P_{HPP} & \text{where category (C): } Q_{HPP} = 450 \text{ m}^3/\text{h} \end{cases}$	2010	550.8

\*In the simulations conducted, the pump selected is in decreasing order of volumetric capacity. For example, a total flow rate of 650 m<sup>3</sup>/h would require one pump from category (B) and one from category (C) [22].

It should be mentioned that for updating the TCI values to the original year, Eq. (B) can be used:

$$\text{Original cost} = \text{cost at reference year} \times \frac{\text{cost index for the original year}}{\text{cost index for the reference year}} \quad (\text{B})$$

In this study, the original year is 2024 and the cost index for this year is 813.9 (the cost index for 2023 year is 797.9 and it is assumed that for 2024 year it is  $1.02 \times 797.9 = 813.9$ ).